



Operational experience and performance evaluation of some of the system integrity and protection schemes

Makarand Sudhakar Ballal¹ · Amit Ramchandra Kulkarni¹ · Hiralal Murlidhar Suryawanshi¹

Received: 23 February 2020 / Accepted: 7 November 2020 / Published online: 27 November 2020
© Springer-Verlag GmbH Germany, part of Springer Nature 2020

Abstract

An Indian power system is characterized by a conglomeration of ultra-high voltage AC and DC, multi-terminal DC, and extra-high voltage AC transmission networks. It consists of a large distribution network across the country along with conventional generation having Ultra-Mega Power Plants (UMPP) and increasing penetration of Renewable Energy Sources (RES). The System Integrity and Protection Schemes (SIPS) play an important role in maintaining a secure and reliable grid and assists in effective grid management during severe power system contingencies. This paper presents the operational experience of some SIPS implemented in India along with their performance evaluations. The operational experience of three important SIPS, one in the Northern Regional (NR) grid and another two in the Western Regional (WR) grid of India are presented. The drawbacks in existing SIPS are pointed out and an algorithm is proposed to overcome these drawbacks. The performance and effectiveness of the proposed algorithm are evaluated by simulation studies on the 39-bus New England system embedded with an HVDC link in MATLAB/Simulink. Simulation results consummated confirm the authenticity of the scheme in preserving system integrity. Results are validated using Electrical Transient Analyzer Program (ETAP), which is a very powerful design and analysis tool and has an extremely user-friendly interface.

Keywords Keywords Operational Experience · Performance Evaluation · System Integrity and Protection Schemes (SIPS) · Power Swing · Distance Relay

1 Introduction

Power systems complexity is enhancing due to the incorporation of more sophisticated electronics stationed components at the source side due to the penetration of renewable sources. It is also because of FACTS devices allied on the transmission side, STATCOM, and power electronics load linked on the distribution side. This movement forces the power grid to work more frequently at maximum achievable capacity and neighboring stability margin. If the system is exposed to a disruption under such aggravating circumstances, voltage or frequency anxiety is esteem to appear. Thus, the power grid has to be dependent on a wide area as well as local control approaches and schemes to maintain system stability and reliability [1–3]. A contention at any point in complex power systems can aggravate cascade events if not

tackled quickly. Abrupt events, such as fault and disconnection of large load, rattle the balance in the system and cause needless line tripping. Analyses of recent blackouts show that actual data on system conditions can provide operators with a scope to detect and alleviate the cascading outage. The use of brand-new technologies can decrease the risk of large system-wide disturbance and blackout by protecting system integrity under detrimental situations. These techniques are known as System Integrity Protection Schemes (SIPS) or Special Protection Schemes (SPS) or Remedial Action Schemes (RAS). They are designed to detect abnormal system conditions and take attentive corrective actions to maintain system integrity and furnish tolerable system performance [4]. The procedure for designing SIPS in [5] explained the effective trade-off between dependability and security.

The SIPS-based methodology is given in [6] used for improving the security of protection operations and the detection of susceptible points. The procedure to assess the risk of mal-operations of SIPS along with undesirable interactions is described in [7]. With the growing installation of

✉ Makarand Sudhakar Ballal
drmsballal@rediffmail.com

¹ Visvesvaraya National Institute of Technology, Nagpur, Maharashtra, India

Phasor Measurement Units (PMUs) in the grid, there is an endeavor to diagnose and pinpoint a crisis [8]. A computational approach to fault location for power transmission grids is given in [9]. It involves an online stage to submit the waveforms and an offline stage for processing. Frequency and voltage derivatives are important indicators to reflect the degree of disturbances and manifest power system dynamics. The wavelet-based method to obtain the characteristics of frequency and voltage derivatives for disturbance analysis is demonstrated in [10]. Impedance analysis of the transmission line model in [11] determines the current unbalance location and fault indices [12]. A shutdown of an ultra-mega-power project (UMPP) in the western region of India enraged by the operation of protection relay during power swing is described in [13]. In this, a SIPS has been invented to mitigate instability occurred due to an unstable power swing. In [14], fundamental frequency phasors of voltage and current have some aspects which can be used for segregation of power swings and metallic faults. These features were analytically extracted using alternator models considered instability studies. In [13], the effects of asymmetrical power swings on distance relay were examined. It is expressed that, in densely loaded power systems, single-pole tripping of the faulty phase may lead to power swings on healthy phases.

In [14], an approach is described to detect an asymmetrical fault during power swings. The method is deprived on the transient alteration at the fault initiation time that could be well captured by transient monitor refined by the dynamic phasors estimation approach. The estimation of relay security index from the apparent impedance to avert the zone-3 mal-operations of protection relays under sprained conditions using SIPS is explained in [15]. The operating characteristics implemented in the modal current ratio plane are simplified in [16]. But the algorithm is exclusively useful for double-circuit transmission lines. Model predictive control-based strategy is explained in [17], which regularly updates the power set points of the Multi-terminal DC converter stations and alternators to mitigate AC line overloads. This controller is attached to the classical automatic generation control. PMUs rooted fault locator/detector approach has been affirmed for the transmission line. However, the existing SIPS did not incorporate with PMUs. The major contribution of this research paper is the comparative analysis of the results obtained after the operational evaluation of three case studies based on the performance experience of SIPS in India. The analysis is based on simulations of a detailed dynamical model of the system. Shortcomings in the existing SIPS can be overcome by implementing the proposed algorithm. It enables the existing SIPS for correct operation by using time-synchronized (PMU) data. Hence there is no need for any prediction or estimation. Unwanted trippings can be avoided and maintain system integrity. The rest of the paper is organized as follows: The operational evaluations

Table 1 Overview of the Indian power grid [18]

SN	Particulars	Quantity
1	Installed Generation Capacity	378 GW
2	Transmission above 220 kV	381,671 ckm
3	Transformation capacity above 220 kV	791,570 MVA
4	Installed Renewable Energy Capacity	65 GW
5	HVDC Bipolar/B to B systems	11 Nos.
6	Multi-Terminal HVDC	1
7	Operational SIPS	52

of three existing SIPS in India are elaborated in Sect. 2. The proposed algorithm is explained in Sect. 3 to overcome the drawbacks in the existing SIPS. In Sect. 4, the authenticity of the proposed scheme is manifested from the assorted simulation results obtained from a modified IEEE 39-bus system embedded with DC link in MATLAB/Simulink environment. Validation is done by comparing it with the results obtained from the Electrical Transient Analyzer Program (ETAP). Section 5 ends the paper.

2 Motivation

India is one of the biggest producers and consumers of electric power in the world. The Indian Power system in respect of planning and operational intention is segregate into five regional grids. The assimilation of regional grids, and thereby formation of National Grid, gestated in the early nineties. The amalgamation of regional grids began with an asynchronous HVDC back-to-back inter-regional connection facilitating a defined exchange of regulated power. It was consequently graduated to high capacity synchronous attachment among the regions. As of March 2020, the overview of the Indian power grid is tabulated in Table 1. Three major occurrences in the Indian power system motivate the authors to present this article.

2.1 Blackout at CGPL–UMPP India on 13 July 2016

At Mundra, a town of Kutch district in the Indian state of Gujarat, Coastal Gujarat Power Limited (CGPL) operates, control, and maintains 5 units each of 800 MW, the total is 4000 MW called as Ultra-Mega Power Plant (UMPP). It supplies power to three states in western India viz. Rajasthan, Gujarat, and Maharashtra and two states in northern India viz. Punjab and Haryana. On July 13, 2016, an unstable power swing event knocked a complete power failure at CGPL [19]. Figure 1 depicts the single line diagram of this event with disturbances in 400 kV substations. SIPS-1 is devised to tackle under system contingency is shown in Table 2.

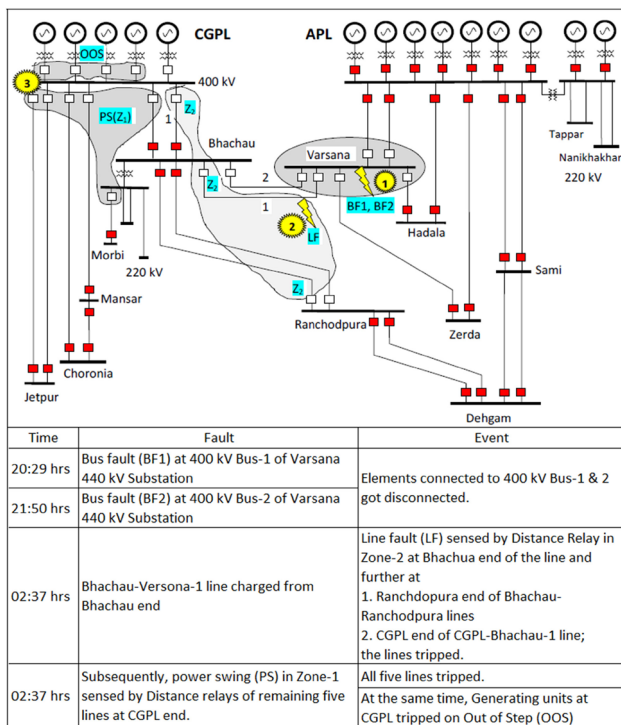
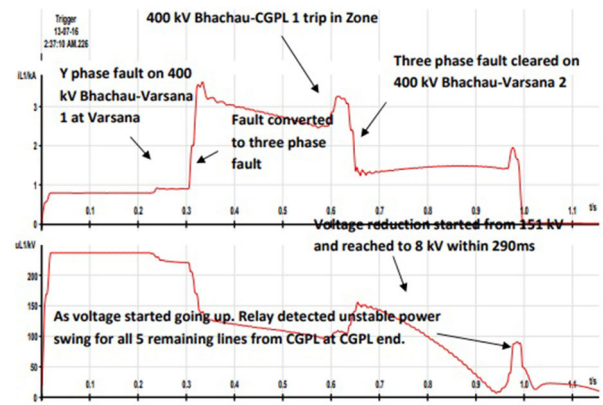


Fig. 1 SLD with history of occurrence at CGPL [19]

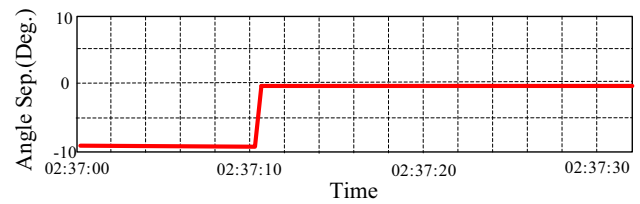
Table 2 Existing SIPS-1 [19]

SN	Triggering Event	Action Plan
1	If exports exceed 3100 MW and any one of the lines trip or if line loading of any line exceeds 900 MW	Reduce the generation of two units to 800 MW
2	If exports exceed 3100 MW and if CGPL-Bachhau double-circuit line trips	Trip one unit immediately
3	If CGPL-Bachhau double-circuit line trips, CGPL-Jetpur or combination of one circuit of each of Bachhau or Choronia or Jetpur trips	Reduce the generation to 800 MW such that the loadings of rest of the lines are below 900 MW

CGPL was submitting 2875 MW in the grid before the occurrence. During the occurrence, two subsequent bus faults on 400 kV bus-1 and bus-2 of 400 kV Varsana substation aggravate these events. Earlier, a bus fault took place at 20:29 Hrs. and the components connected to that bus-1 got disconnected. A consequent fault on bus-2 at 21:50 Hrs caused the desolation of 400 kV Varsana substation. On charging the Bhachau-Varsana-1 line from Bhachau end, a zone-2 line fault was noticed at Bhachua and Ranchodpura end. From the disturbance records, at the time of the incident, the CGPL units were feeding power at Varsana substation. After, 350 ms, there were tripping of 400 kV lines with an unceasing



(a)



(b)

Fig. 2 400 kV CGPL-Bhachau Line 2. a Voltage and current. b Angular Separation at CGPL [19]

downturn of voltage for 290 ms. A rise in voltage was examined eventually at CGPL end as a power swing impinges in its zone-1 of all rest of the lines distance relays. This results in the tripping of relays. It results in unstable power swing as the oscillations were not damped. Thereafter, Out of Step (OOS) protection activated for alternators at CGPL. This leads to a generation loss of 2875 MW. Figure 2a illustrates the pre-fault and post-fault voltage and current. It is seen that a 237–95 kV contraction in the phase voltage during the fault. It is also observed that, as soon as the 400 kV CGPL-Bhachau 1 and 400 kV Bhachau-Ranchodpura twin circuit lines opened, the voltage enhanced to 108 kV at CGPL. Thereafter, even though the fault got cleared, the voltage collapses. Consecutively, even after the clearance of fault from the system, the voltage abstained continuously. Power swing was perceived in all the five lines originating from CGPL. Figure 2b shows angular separation at the time of the incident.

The observation regarding transient stability studies done by an expert study group is available in [19]. The following are the suggestions given by this study group. (i) Line differential protection recommended as critical fault clearance time for the complete network is 100 ms. (ii) Power swing impinging distance relay zone settings on instances of fault are quite more. (iii) Simulation studies in the event of unstable power swing demonstrate that tripping of one of the CGPL units alleviates the oscillations to that end fault

Table 3 Existing SIP-2 [19]

SN	Triggering Event	Action Plan
1	If blocking of one pole and decrement in power submission at Mahendergarh between 600 MW - 900 MW	Load Shedding 300 MW in NR Haryana (150 MW), Punjab (50 MW), Rajasthan (50 MW) and Uttar Pradesh (50 MW)
2	If blocking of one pole and decrement in power submission at Mahendergarh between 900 MW - 1250 MW	Load Shedding 600 MW in NR Haryana (300 MW) along with Punjab, Rajasthan and Uttar Pradesh 100 MW each
3	If blocking of one pole and decrement in power submission at Mahendergarh between 1250 MW - 2000 MW	Load Shedding 1400 MW in NR Haryana (600 MW) along with Punjab, Rajasthan, Uttar Pradesh and Delhi 200 MW each
4	If blocking of both poles and decrement in power submission at Mahendergarh by more than 2000 MW	Load Shedding 1900 MW in Haryana (700 MW) along with Punjab, Rajasthan, Uttar Pradesh and Delhi 300 MW each

clearance by 300 ms. (iv) Existing special protection scheme needs to be modified. After the 2012 Indian blackout, the task force had advocated tripping the line and block tripping of all other zones during power swing if the power swing enters zone-1 characteristics.

2.2 Tripping of ± 500 kV HVDC line on January 8, 2016

India's first HVDC bipolar 2500 MW, 500 kV, 960 km line is in private hands. This link traverse between the Mundra in the western region (WR) to industrial load centers Mohindergarh in the northern region (NR). The SIPS is devised to deal with a contingency for this HVDC system shown in Table 3. It performs two actions one for generation backing down at Mundra-stage 3 (WR) and another action comprises of load shedding of identified loads in NR. This bipolar HVDC link tripped on January 8, 2016, at 6:40 Hrs. Before tripping, the power flow on each pole was 900 MW and the power import at Mohindergarh was 1800 MW. The variation in power is shown in Fig. 3a. The system frequency observed at Mundra fluctuates from 49.73 to 49.98 Hz shown in Fig. 3b. The rise in frequency from 49.85 to 49.95 Hz indicates net load loss during this event. Voltage variations continue for 10 s.

Due to the sudden loss of load in NR, the angular separation between Dehgam in WR and NR decreased by 10 degrees as indicated by the PMU plot in Fig. 3c. Due to the loss of the HVDC link, the power flow on adjacent 765 kV lines is increased. The SIPS devised for the HVDC link came

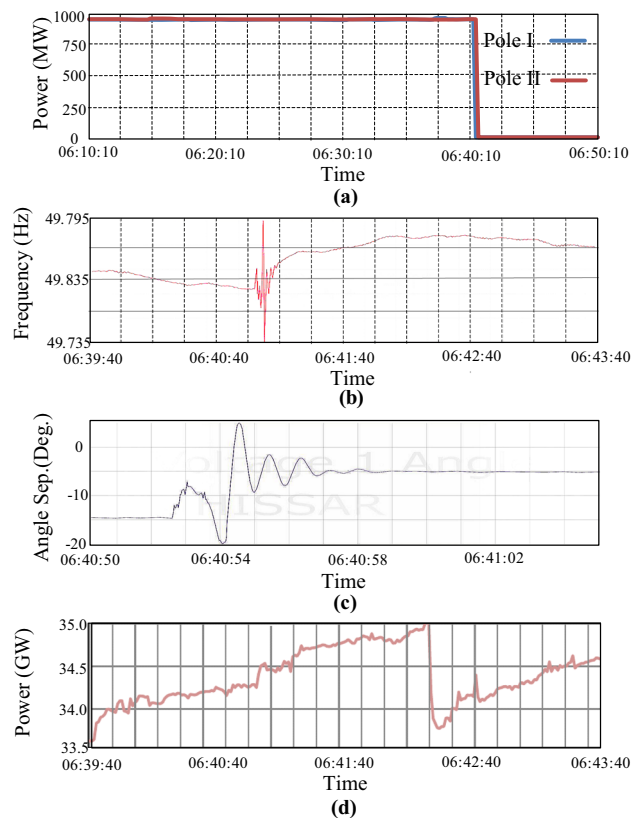


Fig. 3 Operation of SIPS 2. **a** Power flow variation due to HVDC pole tripping. **b** Frequency variation at CGPL-Mundra PMU. **c** Angular separation. **d** Load shedding in NR

into action for safe and reliable operation of the grid during this incidence. As per the SIPS design, if there is a loss of bipolar link, there will be tripping of two generating units and backing down of the third unit at Mundra. In addition to this, 1400 MW load-shedding imposed in NR shown in Fig. 3d. Correct operation of SIPS-2 is observed after this event in WR and NR.

2.3 Tripping of 765 kV double-circuit line between WR and NR on January 14, 2016

765 kV Agra-Gwalior line had been envisaged as a part of the superpower highway comprising of 765 kV Sipat (WR)-Seoni (WR)-Bina (WR)-Gwalior (WR)-Agra (NR)-Fatehpur (NR)-Sasaram (NR)-North Karanpura (ER)-Sipat (WR) 765 kV Agra-Gwalior-Bina. It is operated at 400 kV was commissioned on 31 March 2007 and provided a synchronous inter-regional link between the NR and WR grid. The availability of PMU at 400 kV/765 kV substations/power stations along with a robust fiber optic communication network will facilitate situational awareness, regulation, and control of power flow to sustain grid parameters. SIPS-3 is devised at Gwalior (WR) for corrective actions in the event

Table 4 Existing Special Protection Scheme (SIP-3) [19]

SN	Triggering Event	Action Plan
1	If import by NR is between 1500–1000 MW on 765 kV Agra-Gwalior Circuit 1& 2	Reduce the generation of two units to 520 MW
2	If import by NR is more than 1500 MW on 765 kV Agra-Gwalior Circuit 1and 2	Load Shedding 1145 MW in NR

of harsh contingency to prevent grid disturbances expressed in Table 4.

On the early morning of January 14, 2016, there was dense fog in northern parts of India and various 400 kV lines were under outages. HVDC link Mundra – Mohindergarh was operating in reduced voltage mode with flow restricted to 1000 MW. At 07:14 Hrs, 765 kV Gwalior-Agra Circuit-2 tripped due to earth fault on Y phase as indicated by Agra PMU. Voltage dipped at 155 kV momentarily from an initial value of 430 kV. This tripping increased power flow on 765 kV Gwalior-Agra Circuit-1 to 2300 MW. At 07:30 Hrs, 765 kV Gwalior-Agra Circuit-1 also tripped on the earth’s fault on the Y phase. The maximum voltage dip was observed in Y phase shown by 400 kV Agra PMU. Due to the tripping, there was a rise in angular separation from 17° to 34° between Bina (WR) and Agra (NR) substations. Subsequently, SIPS came into operation and there was load shading of 1200 MW in the states of Punjab, Haryana, UP, Rajasthan of NR. Generation backing down occurs in WR at Mundra by 180 MW, Korba Thermal Power Station (KTPS) Unit-7 by 145 MW, and Vindhyachal Stage 3 by 250 MW as accomplish in SIPS-3.

The complete operation of SIPS-3 under this contingency is depicted in Fig. 4. From the performance analysis of these three SIPS, it is observed that power swing appears in all the lines. From the above analysis, it came to know that SIPS operates correctly in the latter two incidences, and in the first incidence, the entire blackout took place at CGPL Mundra. To avoid such unwanted blackouts in the future, existing SIPS are improved by incorporating the proposed algorithm. This algorithm is discussed in the following section.

3 Proposed algorithm for correct operation of existing SIPS

In a part of power system shown in Fig. 5, a line is connecting between to buses, real-time voltage $v(t)$ and current signals $i(t)$ of both ends (i and j) are measured by PMUs. The RMS values of the voltages (V_i and V_j) and currents (I_i and I_j) and their respective phase angles (θ_i and θ_j) are determined by

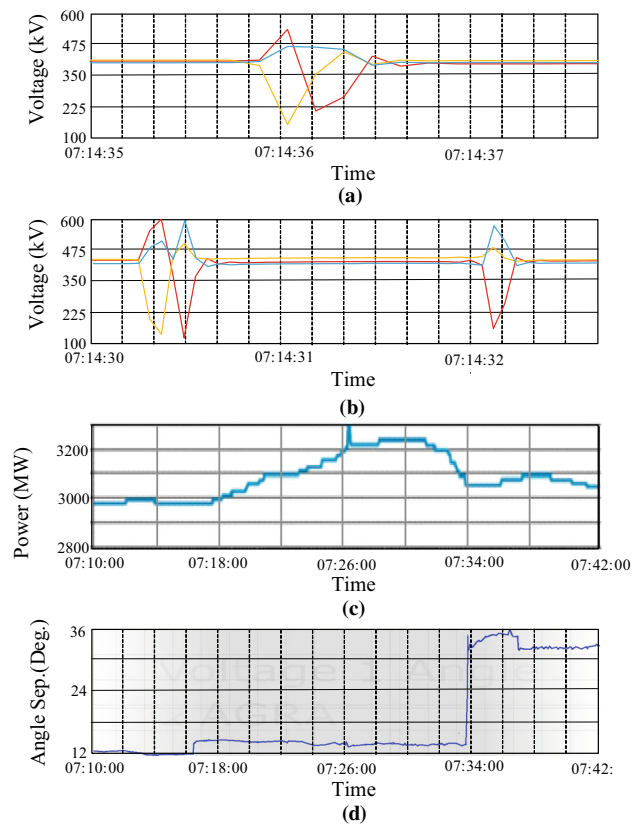


Fig. 4 Operation of SIPS-3 Voltage dip after tripping of 765 kV Gwalior-Agra. **a** Circuit 1. **b** Circuit 2 and **c** Generation back down at CGPL-Mundra. **d** Angular separation observed by Agra PMU

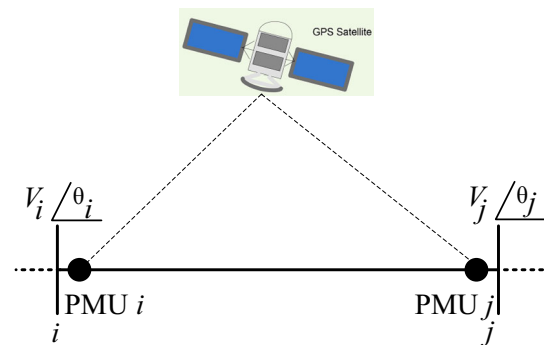


Fig. 5 Application of PMU for system awareness

three sample technique. The differential voltage and current are calculated as

$$\Delta V_{ij-abc} = V_{i-abc} - V_{j-abc} \tag{1}$$

$$\Delta I_{ij-abc} = I_{i-abc} - I_{j-abc} \tag{2}$$

During only a power swing, ΔI_{ij-a} , ΔI_{ij-b} and ΔI_{ij-c} are equal to zero.

$$\Delta I_{ij-a} = \Delta I_{ij-b} = \Delta I_{ij-c} = 0. \tag{3}$$

During a power swing and in case of phase-*a* to ground fault ΔI_{ij-b} and ΔI_{ij-c} are only equal to zero. However, the ΔI_{ij-a} is not equal to zero. This difference is used to select the faulty phase. The change in impedance seen by the relay at the end *i* is expressed as

$$\Delta Z_{ij-abc} = \frac{\Delta V_{ij-abc}}{I_{i-abc}} \tag{4}$$

Only during a power swing, the rate of change of impedance Z_{ij-abc} is zero for a defined period *T*.

$$\Delta Z_{ij-a} = \Delta Z_{ij-b} = \Delta Z_{ij-c} = 0. \tag{5}$$

Phase angle discrepancies from PMU are entrenched as important quantity for expeditious monitoring, following to any unwilling outage circumstance. The angular separation of voltage phasors from PMUs is used in this work as an early indicator of system stability. The angular separation between both ends (*i* and *j*) is given as

$$\delta_{ij-abc} = \theta_{i-abc} - \theta_{j-abc}. \tag{6}$$

During only a power swing, $\delta_{ij-a}, \delta_{ij-b}$ and δ_{ij-c} are equal.

$$\delta_{ij-a} = \delta_{ij-b} = \delta_{ij-c}. \tag{7}$$

During a power swing and in case of phase-*a* to ground fault, δ_{ij-b} and δ_{ij-c} will be equal. However, the angle δ_{ij-a} is less than δ_{ij-b} and δ_{ij-c} . The comparison of the rate of change of δ_{ij-abc} with its predefined minimum value for a defined time interval *T* has been used to identify power swing. This indicates a stable power swing. It is given as,

$$\Delta \delta_{ij} \geq \Delta \delta_{ij(\min)} \dots t \leq T. \tag{8}$$

δ_{ij} is obtained by taking the average of $\delta_{ij-a}, \delta_{ij-b}$, and δ_{ij-c} . If the rate of change of δ_{ij} is greater than its predefined value for more than defined time interval *T*, it will indicate an unstable power swing. It is expressed as,

$$\Delta \delta_{ij} \geq \Delta \delta_{ij(\min)} \dots t \geq T. \tag{9}$$

From (4), the change in impedance observed by the relay is compared with the threshold values set for all three zones. The threshold value for zone-1, zone-2 and zone-3 are $\Delta Z_1, \Delta Z_2$, and ΔZ_3 respectively. There might be a possibility that the impedance ΔZ_{ij} can be less than set threshold values if power swing occurs. Therefore, to discriminate against the condition of fault and power swing, the change in current ΔI_{ij} is determined from (2). If this change in current equal to zero means there is no fault in line but the change in impedance seen by the relay ΔZ_{ij} is due to power swing. This feature is incorporated in protection relays to avoid false tripping.

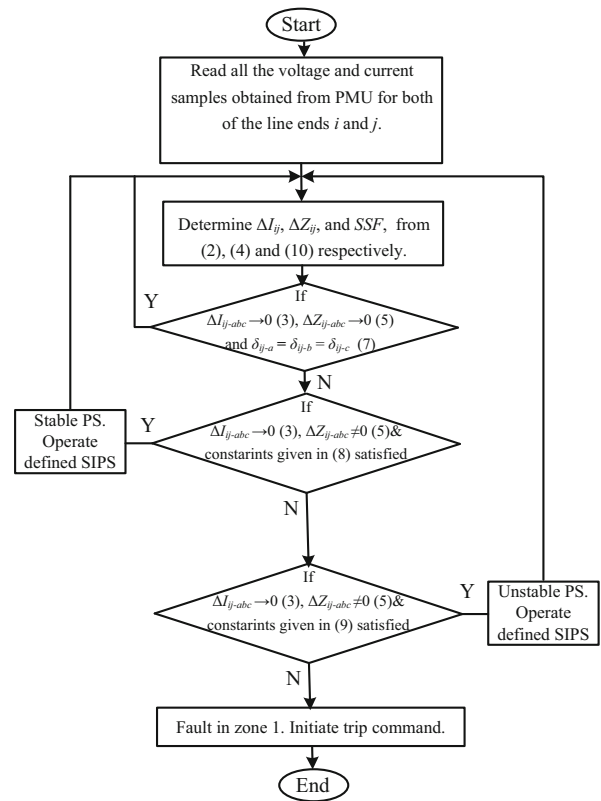


Fig. 6 Flow chart of the proposed algorithm

The system stability factor is defined as a difference of maximum angular separation $\delta_{ij(\max)}$ and actual δ_{ij} .

$$SSF = \delta_{ij(\max)} - \delta_{ij}. \tag{10}$$

The existing SIPS algorithms are modified in the light of (1)–(10). The flow chart of proposed the algorithm is given in Fig. 6. Initially, it read all the voltage and current samples obtained from PMU for both of the lines end *i* and *j*. Thereafter, it determines $\Delta I_{ij}, \Delta Z_{ij}$, and *SSF*, for time period *T* from (3), (4), and (10), respectively. The next task is that the algorithm checks the predefined conditions. If ΔI_{ij-abc} equal to zero as given in (3), ΔZ_{ij-abc} also equal to zero as given in (5) and $\delta_{ij-a}, \delta_{ij-b}$ and δ_{ij-c} are equal as given in (7), it indicates the healthy or normal condition. Thus, the algorithm regains start from the earlier step; otherwise, it will go to the next step.

If ΔI_{ij-abc} approaches to zero, but ΔZ_{ij-abc} not equal to zero, and constraint given in (8) is satisfied. It indicates a stable power swing condition. Thus, the algorithm operates the respective subroutine of SIPS and thereafter it starts from the initial step. In case, if ΔI_{ij-abc} equal to zero, but ΔZ_{ij-abc} not equal to zero, and constraint given in (9) is satisfied. It indicates an unstable power swing condition. Thus, the algorithm operates the corresponding subroutine of SIPS and starts from the initial step. If ΔI_{ij-abc} and ΔZ_{ij-abc} are

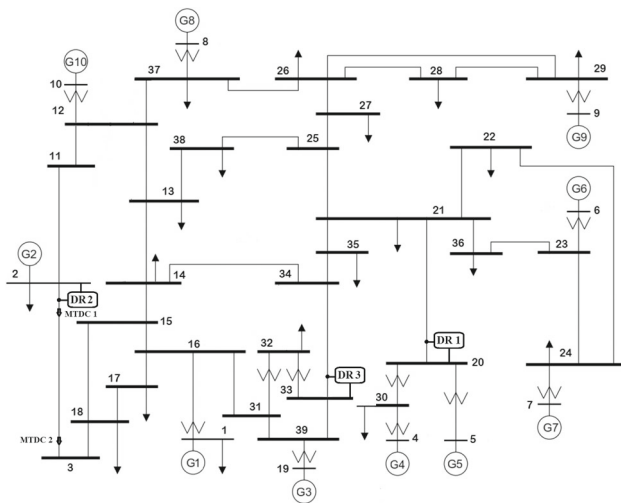


Fig. 7 IEEE 39-bus New England system embedded with a HVDC link

not equal to zero and constraints given in (8) or (9) are satisfied. It could be a stable or unstable power swing condition with a fault in zone-1. Therefore, the algorithm initiates trip commands to the respective circuit breaker and jumps to the beginning stage. The performance evaluation is discussed in the following section.

4 Performance evaluations of some of the existing SIPSs with proposed algorithm

The above response of three SIPS is meticulously verified on the IEEE 39-bus New England system shown in Fig. 7. A multi-terminal DC (MTDC) system has more than two converter stations is embedded in the New England 39-bus test system. All AC transmission lines are modeled using a lumped π model. The algorithm is developed in MATLAB[®]; these systems are modeled in the ETAP environment and are confirmed by commensuration with the load flow results. The current and voltage samples from the secondary side of CT's and CCVT's are obtained by using a second-order low-pass Butterworth filter. The entire cycle recursive discrete Fourier transform (DFT) is used to calculate the voltage and current phasors. The operational performances of three SIPS are evaluated on the distance relays DR1, DR2, and DR3, respectively.

4.1 Performance evaluation of SIPS-1

Testing of SIPS is carried out to check its capability if it forbids system instability under normal and stressed system conditions. The relay at bus 19 online L-22 is quoted as Test Relay 1 (DR1) fix for its safeguard operation during volt-

age stress, load encroachment, and power swing. Further, the inflated zone-2 operation is validated for symmetrical three-phase faults in the zone-2 of the DR1. This SIPS-1 is checked under different system contingency conditions.

4.1.1 Performance evaluation of SIPS-1 under stable power swing condition

The symmetrical three-phase fault is enforced at 1 s in the line L-24 between bus 16 and bus 24. The fault at both ends cleared in 90 ms after the opening of the circuit breaker. As an effect of the three-phase fault exercised, the distance relay DR1 detects a power swing. The waveforms of voltage and current indicate a stable power swing and the angular separation of generation rotor angles along with the stability curve depicted in Fig. 8a.

4.1.2 Performance evaluation of SIPS-1 under unstable power swing condition

The symmetrical three-phase fault is imposed at 1 s in the line L-24 and opening of the circuit breaker at both ends within 260 ms clears the fault. Distance relay DR1 detects power swing. An unstable power swing is indicated by the voltage and current waveforms. The angular dissociation between rotor angles of alternators and repeated oscillations pinpoint unstable power swing as given in Fig. 8b.

In the existing logic, the power swing blocking scheme is marked to be altered from 'block all zones except zone-1' on power swing revelation to 'block all zones'. However, this SIPS-1 failed due to the power swing observed in zone-1 of all the five lines emanating from CGPL. This swing enters in zone-1 because of a delay in a curtailment in the faulty section. Therefore, modification is suggested in the existing SIPS-1 is given in the following subsection.

4.1.3 Performance evaluation of SIPS-1 with proposed algorithm

With the improvement in measurement technologies, the outright rotor angle is now assessable using the PMU signal as input and is declared to be useful in correcting power system vigorous performance. For an aberrant contingency, the eminence of the generation angle and its change are higher than a balanced contingency. For (i and j) the given system, an unstable squabble is detected if the angular displacement is greater than 28.1° or $\pi/6.4$ radians. It illustrates that the system is near instability, curative actions are originated and the system instability is annexed. While ratifying this reformed scheme, it has been taken care to secure that the protection relay is encouraged for the operation of every fault during power swing. Distance relay operation of all zones for lines 20–21, 21–22, and 22–24 are blocked after the detection of

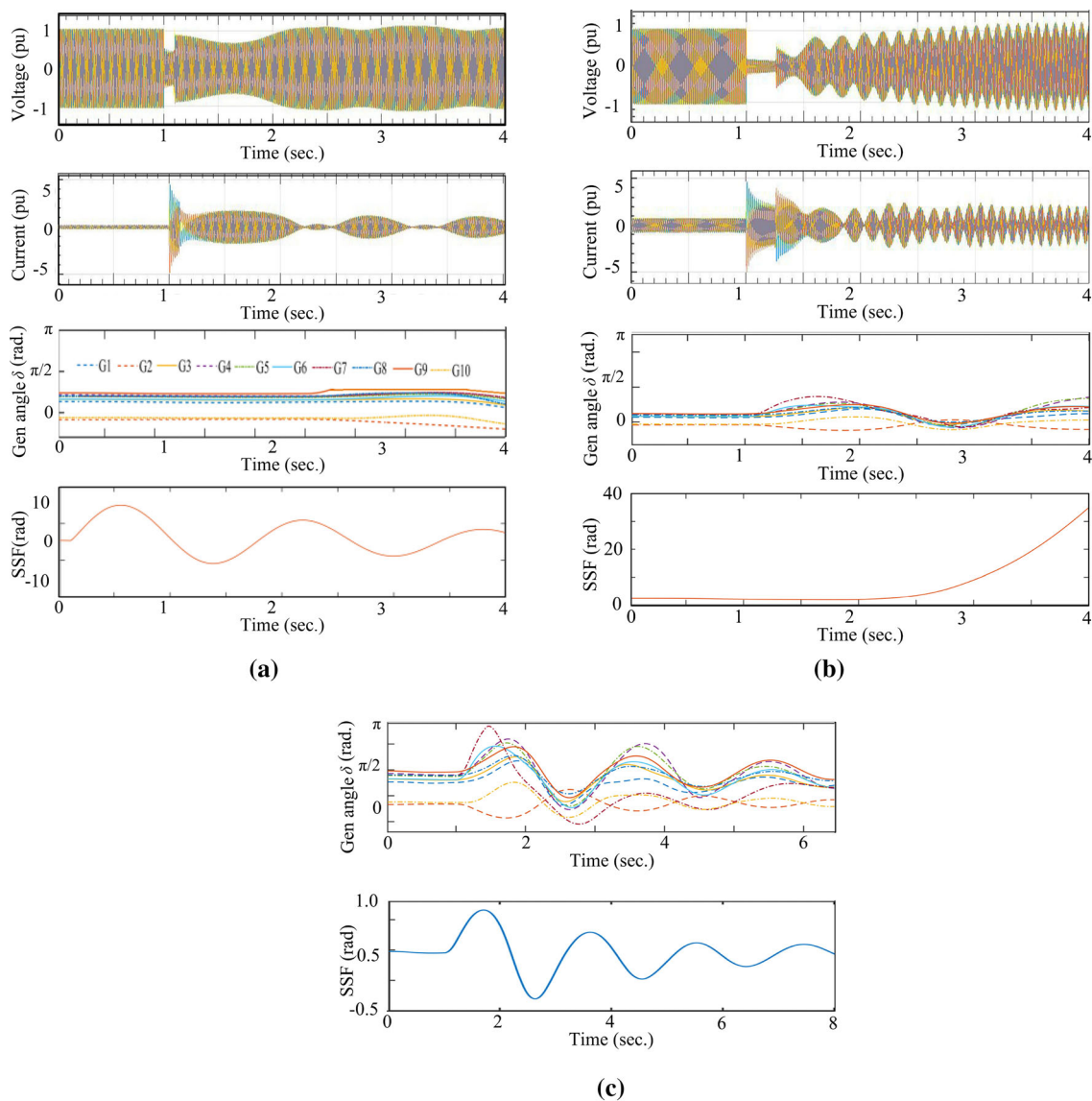
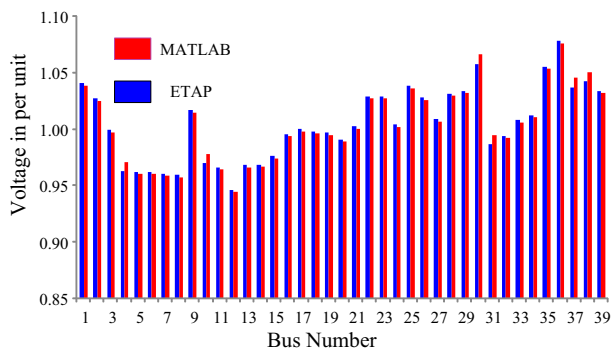


Fig. 8 Performance evaluation of SIPS-1 **a** under stable power swing, **b** under unstable power swing and **c** with proposed algorithm

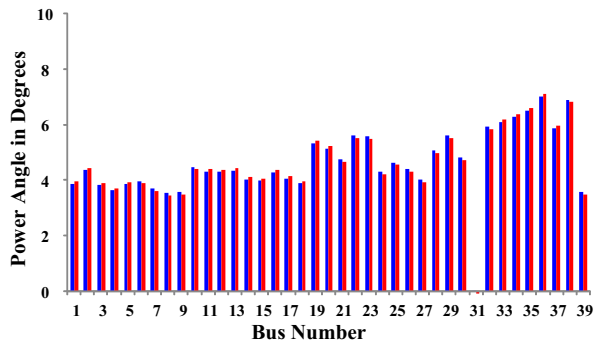
power swing. Now, the symmetrical fault is applied on lines 22–24 while power swing, at 2 s. This fault is cleared after 85 ms. Relay DR1 detects a fault in zone-3 during power swing. This feature is incorporated in the existing SIPS-1 at the start and based on *SSF* the corresponding lines distance relays are blocked or de-blocked. The relay DR1 remains in block condition and the generation G5 is reduced in proportion to the power flow through lines 22–24. This mitigates the power swing and the system acquires stable condition as shown in Fig. 8c.

Electrical Transient Analyzer Program (ETAP) was flourished by Operation Technology, Inc., USA since 1986. It has capabilities like transient stability analysis with a user-friendly interface. It can be used to model control systems by

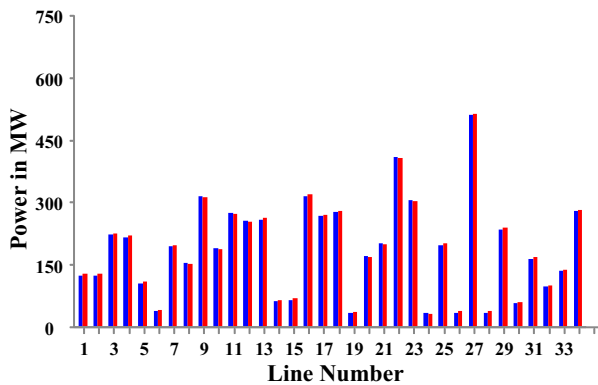
third party software [20]. In this article, ETAP is used for validation of results obtained by MATLAB/Simulink. Results demonstrated by both are compared with each other. The proposed algorithm was evaluated over an IEEE 39-bus New England system embedded with an HVDC link. The bus voltage, power angle, and line power are illustrated in Fig. 9 for the normal operating condition. The 31st bus to which G2 is connected is taken as a reference bus and thus the power angle for this bus is zero. The voltage noticed by MATLAB and ETAP is 0.992 pu and 0.989 pu, respectively. Active power flows are also matching closely. Figures 10 and 11 give the results after a disturbance with and without application of the proposed algorithm, respectively. It can be seen from Fig. 11 that there is a noticeable change in voltage and



(a)



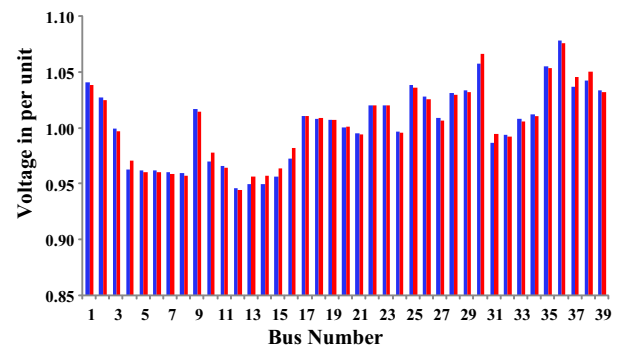
(b)



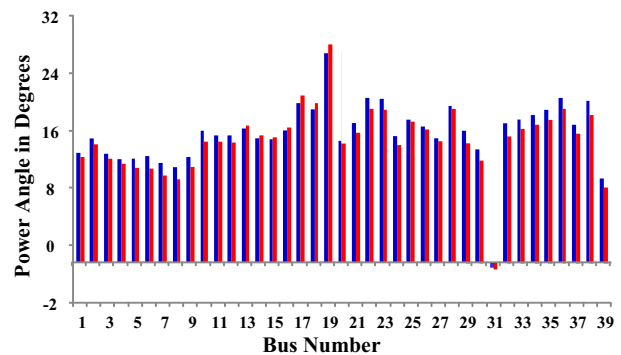
(c)

Fig. 9 IEEE 39 Bus system under normal condition **a** bus voltage, **b** power angle and **c** line power

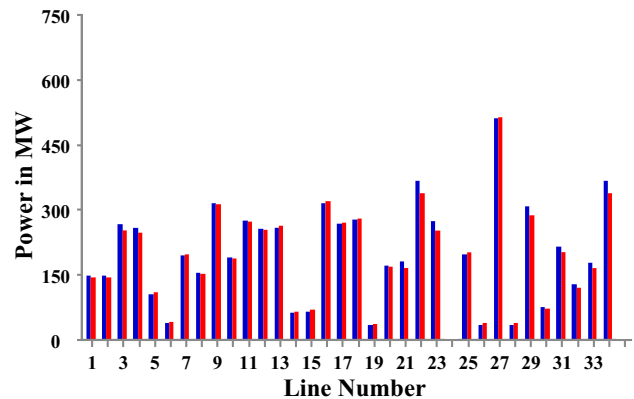
power angle of bus 16, 19, 23, and 24 due to interruption of line L-24. The power angle of bus 19 is approaching 30° . The system rushed toward instability. The active power of L-24 became zero. This may cause unwanted tripping of line L-22. But, due to the application of the proposed algorithm, the Relay DR 1 was locked and protection relays on lines L-20, L-21, L-22 and L-24 are de-blocked. As the fault is noticed in zone-1 of line L-24, the protection of this line operates from both ends. Thus, the power of L-24 is zero but the voltage and power angle sets at a better value. The power swing



(a)



(b)



(c)

Fig. 10 IEEE 39 Bus system after fault without application of proposed algorithm **a** bus voltage, **b** power angle and **c** line power

was observed for a while and it mitigates quickly. Thus, the system acquires a stable condition.

4.2 Performance evaluation of SIPS-2 with proposed algorithm

A symmetrical fault is applied at 1.2 s in the DC line L-15 joined bus 9 and bus 39. The circuit breaker opening at both ends in 80 ms clears the fault. As an effect of the symmetrical fault applied, the test relay DR2 diagnoses a power swing.

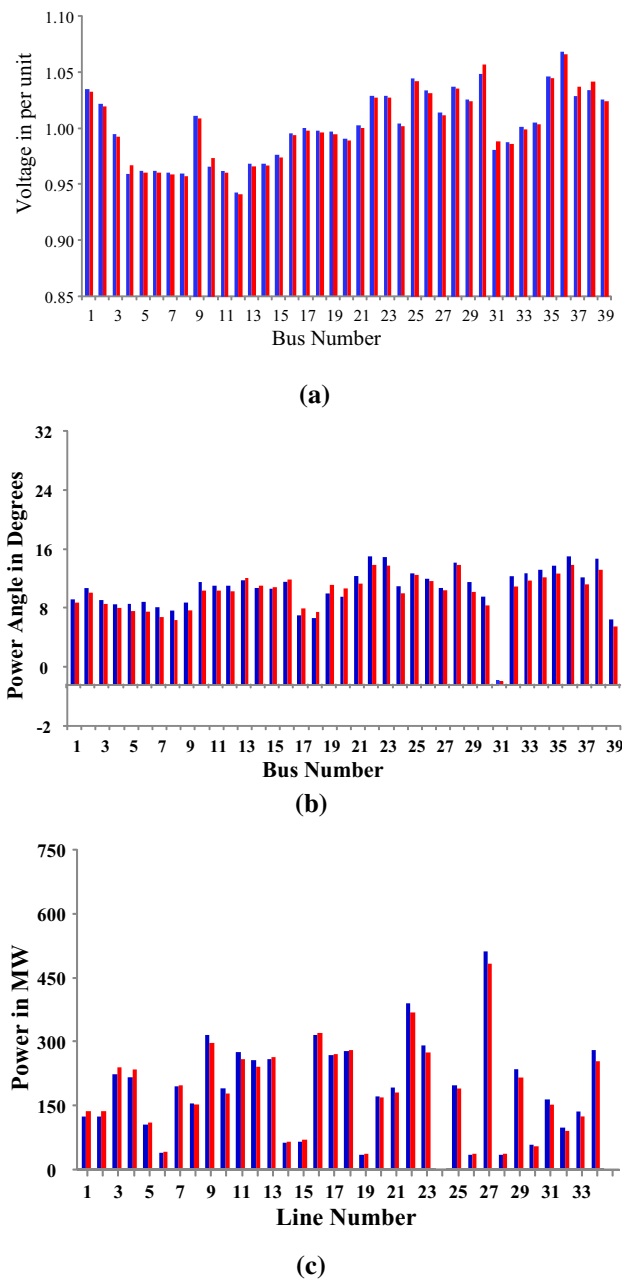


Fig. 11 IEEE 39 Bus system after fault with application of proposed algorithm **a** bus voltage, **b** power angle and **c** line power

The performance of this SIPS-2 is shown in Fig. 12. The angular segregation of generation rotor angles along with the stability curve is seen. The SIPS-2 comes into operation and the load connected to bus 8 is curtailed.

With regards to the comparison of MATLAB and ETAP, the results were very close in all of the plots. The voltage and power angle at bus 9 was dropped and increased, respectively. However, the voltage at bus 39 improved by 0.2 pu and there is no significant change in power angle. Due to the application of the proposed algorithm, there was not only curtailment of

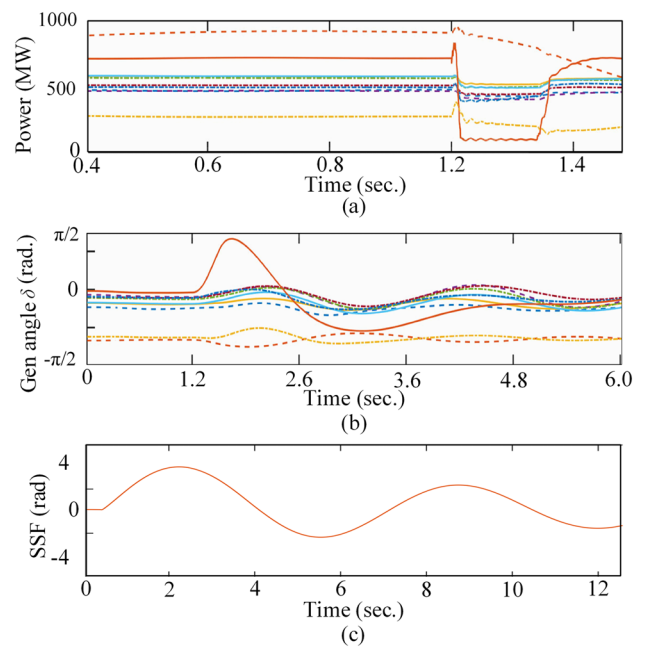


Fig. 12 Performance evaluation of SIPS-2 when associated with proposed algorithm

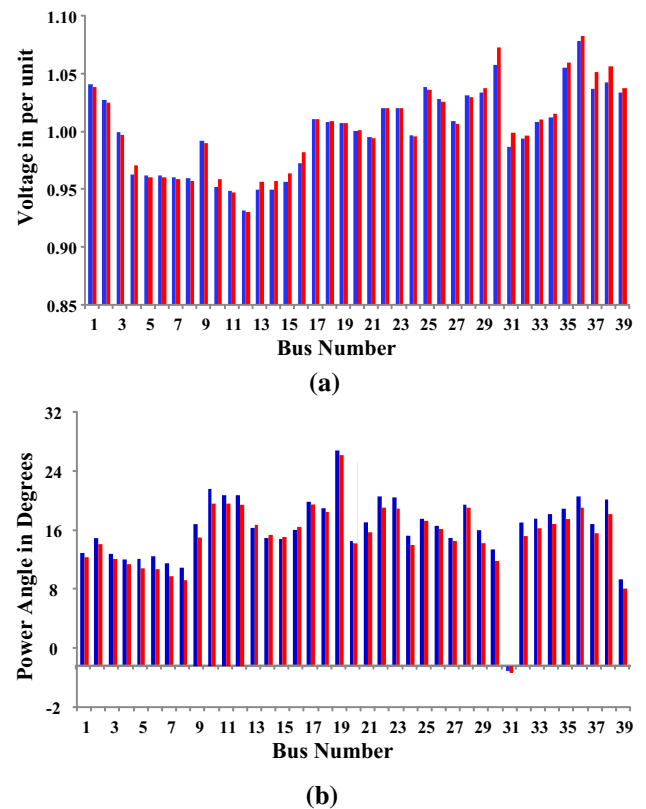


Fig. 13 IEEE 39 Bus system after fault without application of proposed algorithm **a** bus voltage, and **b** power angle

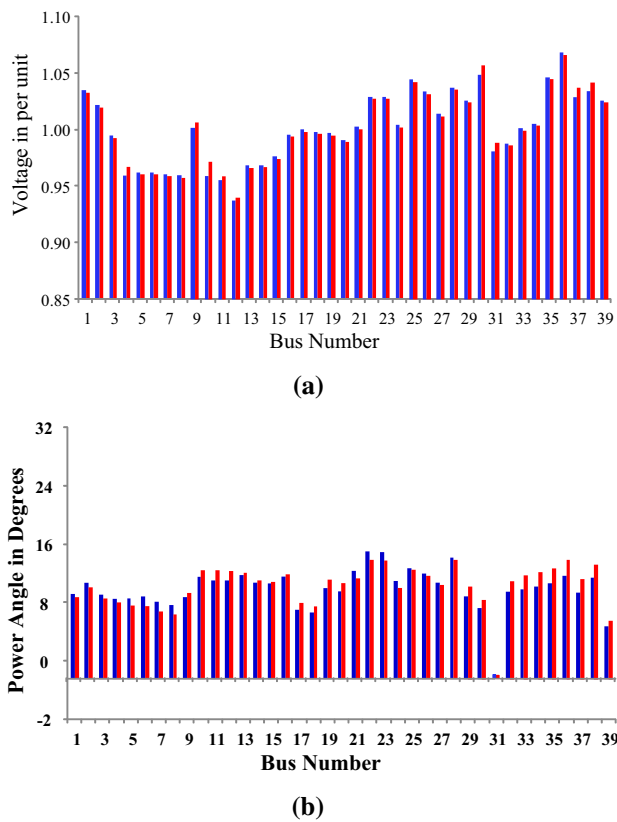


Fig. 14 IEEE 39 Bus system after fault with application of proposed algorithm **a** bus voltage, and **b** power angle

load on bus 8 but also a substantial reduction in power flow from generator G1. This inference was drawn from the results given in Figs. 13 and 14, respectively, for without and with application of the proposed algorithm.

4.3 Performance evaluation of SIPS-3 with proposed algorithm

A symmetrical fault is stimulated at 1.2 s in the line L-21 attached to bus 16 and 17. The opening of the circuit breaker at both bus ends in 85 ms clears the fault. As an effect of the three-phase fault applied, the test relay DR 3 detects a power swing. The performance is shown in Fig. 15. The angular separation of generation rotor angles along with the stability curve is seen. The SIPS3 comes into operation and the load connected to bus 3 and 18 is curtailed. The generation G3 is also reduced in proportion to the curtailed load and the system stability is maintained.

The comparison of MATLAB and ETAP results is given in Figs. 16 and 17, respectively, for without and with the application of proposed algorithm. These results are found close in all the plots. The voltage at bus 17 was dropped and its power angle increased. Whereas, the voltage at bus 16 and 13 were improved and the power angles are a little bit

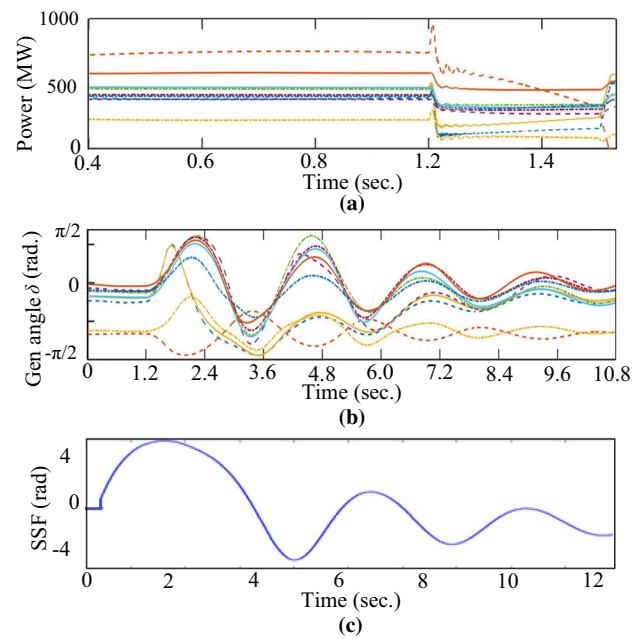


Fig. 15 Performance evaluation of SIPS-3 when associated with proposed algorithm

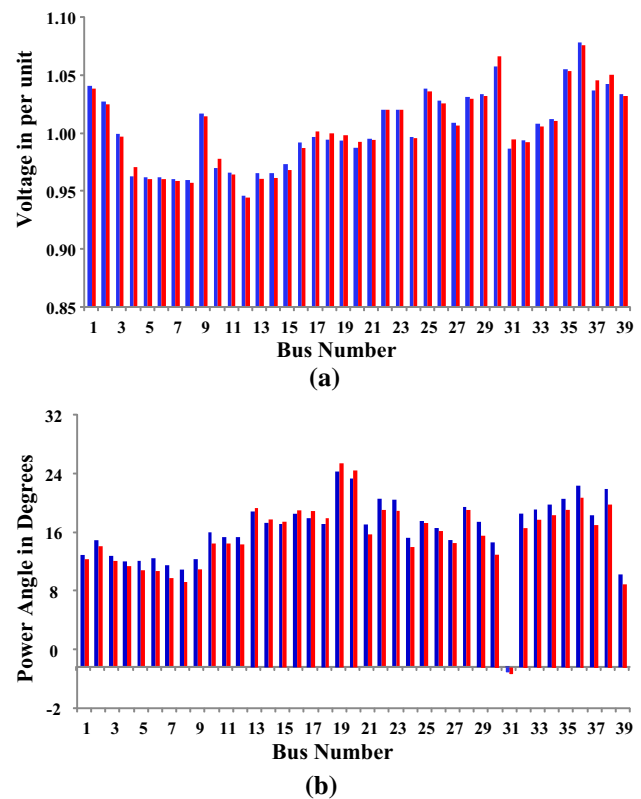


Fig. 16 IEEE 39 Bus system after fault without application of proposed algorithm **a** bus voltage and **b** power angle

reduced. But, due to the application of proposed algorithm, there was an appropriate curtailment of load on buses 3, 18,

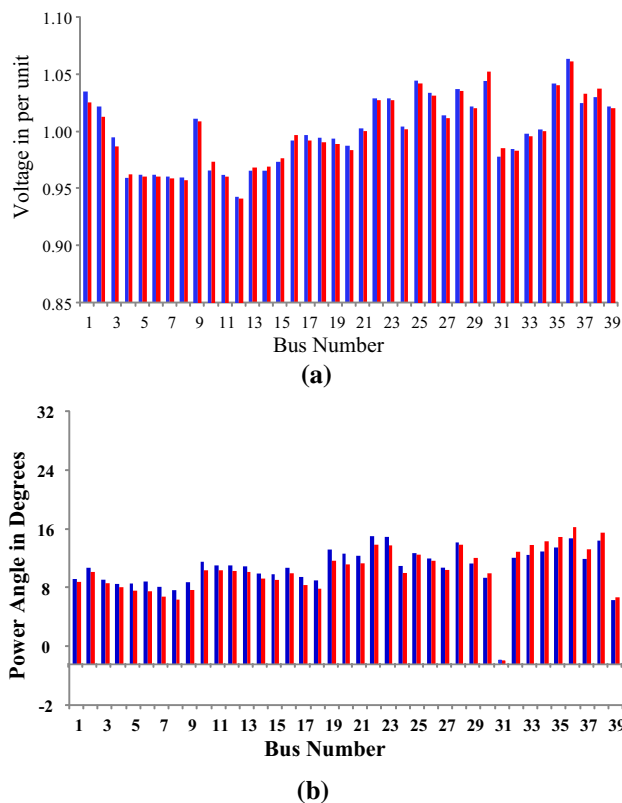


Fig. 17 IEEE 39 Bus system after fault with application of proposed algorithm **a** bus voltage and **b** power angle

and 27 in addition to sufficient reduction in power flow from generator G3. Thus, the system maintains its stability without any delay. The outcomes of this paper are as below.

1. Analysis of three different SIPS is carried out in simulation with the commercially available software on the 39-bus New England system embedded with an HVDC link.
2. Performance evaluation illustrates the cause for the correct or incorrect operation of these SIPS.
3. An algorithm is proposed which requires PMU data to decide on blocking and de-blocking of distance relays so that the existing SIPS could be operated effectively.
4. Proposed scheme does not require any estimation or prediction methodology and it will be more effective for critical application.
5. Results obtained in MATLAB are validated with the results of ETAP and found satisfactory.

5 Conclusion

This paper presents three case studies based on the operational experience of important SIPS in India. The drawbacks

in the execution of existing SIPS are overcome by proposing an algorithm which requires PMU data. The actual time data from PMU will knock out the requirement for complex system modeling and the possibility of potential errors. The algorithm separates the power swing and fault conditions and avoids unwanted tripping. The strenuous simulations executed in MATLAB/Simulink and ETAP over the IEEE 39-bus New England system convince the materiality of the proposed algorithm in assuring system integrity.

References

1. Kundur P (1994) Power system stability and control. McGraw-Hill, New York
2. Yu YN (1983) Electric power system dynamic. Academic Press, New York
3. Taylor CW, Erickson DC, Martin KE, Wilson RE, Venkatasubramanian V (2005) WACS-wide-area stability and Voltage control system: R&D and online demonstration. Proc IEEE 93:892–906
4. Anderson PM, LeReverend BK (1996) Industry experience with special protection schemes. IEEE Trans Power Syst 11(3):1166–1179. <https://doi.org/10.1109/59.535588>
5. Panteli Mathaios, Crossley Peter A, Fitch John (2015) Design of dependable and secure system integrity protection schemes. Int J Electr Power Energy Syst 68:15–25
6. Kundu P, Pradhan AK (2016) Enhanced protection security using the system integrity protection schemes (SIPS). IEEE Trans. Power Delivery 31(1):228–235
7. Liu Nan, Crossley Peter A (2018) Assessing the risk of implementing system integrity protection schemes in a power system with significant wind integration. IEEE Trans Power Delivery 33(2):810–820
8. Kim DI, Chun TY, Yoon S-H, Lee G, Shin Y-J (2017) Wavelet-based event detection method using PMU data. IEEE Trans. Smart Grid 8(2):1154–1162
9. Korkali M, Lev-Ari H, Abur A (2012) Traveling-wave-based fault location technique for transmission grids via wide-area synchronized voltage measurements. IEEE Trans Power Syst 27(2):1003–1011
10. Gao W, Ning J (2011) Wavelet-based disturbance analysis for power system wide-area monitoring. IEEE Trans. Smart Grid 2(1):121–130
11. Chunju F, Xiuhua D, Shengfang L, Weiyong Y (2007) An adaptive fault location technique based on PMU for transmission line. In: Proc. IEEE Power Eng. Soc. Gen. Meeting, Tampa, Florida, USA, pp 1–6
12. Feng G, Abur A (2016) Fault location using wide-area measurements and sparse estimation. IEEE Trans Power Syst 31(4):2938–2945
13. Kumar DS, Savier JS (2019) Synchrophasor based system integrity protection scheme for an ultra-mega power project in India. IET Gener Transm Distrib 13(8):1220–1228
14. Hashemi SM, Sanaye-Pasand M, Shahidehpour M (2018) Fault detection during power swings using the properties of fundamental frequency phasors. IEEE Trans Smart Grid 10(2):1385–1394
15. Gawande P, Dambhare S (2019) New predictive analytic-aided response-based system integrity protection scheme. IET Gener Transm Distrib 13(8):1204–1211

16. Unde S, Gawande P, Dambhare S (2019) New algorithm for protection of double circuit transmission lines using modal currents. *IEEE Trans. Power Deliv* 34(5):1967–1977
17. Mehrbankhomartash M, Saeedifard M, Grijalva S (2019) Model predictive control-based AC line overload alleviation by using multi-terminal DC grids. *IEEE Trans Power Syst* 35(1):177–187
18. Annual Report 2019–20, Power Grid Corporation of India Limited. Available at https://www.powergridindia.com/sites/default/files/NSE_AR_dt29082020.pdf
19. W. R. P. Committee. Minutes of 35th meeting of wrpc. 2018. Available at http://www.wrpc.gov.in/wrpc/35wrpc_minutes.pdf
20. E-Tap 7.0.0 Demo Guide by Operation Inc. Available at <https://etap.com/demo-download>

Publisher's Note Springer Nature remains neutral with regard to jurisdictional claims in published maps and institutional affiliations.